Microbiology:

The Universal Epitope of Influenza A Viral Neuraminidase Fundamentally Contributes to Enzyme Activity and Viral Replication

Tracey M. Doyle, Bozena Jaentschke, Gary Van Domselaar, Anwar M. Hashem, Aaron Farnsworth, Nicole E. Forbes, Changgui Li, Junzhi Wang, Runtao He, Earl G. Brown and Xuguang Li

J. Biol. Chem. 2013, 288:18283-18289.
doi: 10.1074/jbc.M113.468884 originally published online May 3, 2013

THE JOURNAL OF BIOLOGICAL CHEMISTRY VOL. 288, NO. 25, pp. 18283–18289, June 21, 2013

The Universal Epitope of Influenza A Viral Neuraminidase Fundamentally Contributes to Enzyme Activity and Viral Replication*

Received for publication, March 12, 2013, and in revised form, April 14, 2013 Published, JBC Papers in Press, May 3, 2013, DOI 10.1074/jbc.M113.468884

Tracey M. Doyle[‡§1], Bozena Jaentschke[‡], Gary Van Domselaar[¶], Anwar M. Hashem[‡§‖2], Aaron Farnsworth[‡], Nicole E. Forbes[§], Changgui Li[**], Junzhi Wang[**], Runtao He[¶], Earl G. Brown[§], and Xuguang Li[‡§3]

From the [‡]Centre for Vaccine Evaluation, Biologics and Genetic Therapies Directorate, Health Products and Food Branch, Health Canada, Ottawa, Ontario K1A 0K9, Canada, [¶]National Microbiology Laboratory, Public Health Agency of Canada, Winnipeg, Manitoba R3E 3R2, Canada, [‖]Department of Medical Microbiology and Parasitology, Faculty of Medicine, King Abdulaziz University, Jeddah, Saudi Arabia, [**]National Institutes for Food and Drug Control, Beijing 100050, China, and [§]Department of Biochemistry, Microbiology and Immunology and Centre for Emerging Pathogens Research, University of Ottawa, Ottawa, Ontario K1H 8M5, Canada

Background: The influenza viral neuraminidase has only one universally conserved peptide sequence with unknown function.
Results: Sequence alterations in this region decrease substrate binding, enzymatic activity, protein stability, and viral growth.
Conclusion: The universal epitope is indispensable for maximal enzymatic function and robust viral propagation.
Significance: The universally conserved NA sequence is an attractive target for antiviral intervention and vaccine development.

The only universally conserved sequence among all influenza A viral neuraminidases is located between amino acids 222 and 230. However, the potential roles of these amino acids remain largely unknown. Through an array of experimental approaches including mutagenesis, reverse genetics, and growth kinetics, we found that this sequence could markedly affect viral replication. Additional experiments revealed that enzymes with mutations in this region demonstrated substantially decreased catalytic activity, substrate binding, and thermostability. Consistent with viral replication analyses and enzymatic studies, protein modeling suggests that these amino acids could either directly bind to the substrate or contribute to the formation of the active site in the enzyme. Collectively, these findings reveal the essential role of this unique region in enzyme function and viral growth, which provides the basis for evaluating the validity of this sequence as a potential target for antiviral intervention and vaccine development.

Influenza A is an enveloped virus containing a segmented negative-sense RNA genome. The viral envelope contains two major glycoproteins, hemagglutinin (HA) and neuraminidase (NA)[4] of which there are at least 17 and 10 subtypes, respectively (1–3). Although HA has been well characterized to be essential for entry into host cells, the functional roles of NA in viral replication are less well understood. Previous reports suggest that NA exerts its functional role during viral exit from the cell. Specifically, NA enzymatically cleaves sialic acid, the influenza host cell receptor, and facilitates the release of viral particles that allows them to infect additional cells (4–6). Indeed, this role is supported by the observation that NA-defective virus or wild type viruses in the presence of NA inhibitors form aggregations on the apical surface of the cells (7–9). Furthermore, NA has been suggested to play additional roles in viral infection including mucus breakdown, which allows for increased viral diffusion throughout the respiratory tract during infection (10, 11) and more recently has been shown to contribute to the entry and fusion of the influenza virus into host cells (12, 13). It is also noteworthy that the viral neuraminidase may increase bacterial adherence after viral preincubation, predisposing the patients to secondary bacterial infection (14), which is one of the most common causes of fatality in influenza patients (15, 16).

Because of the importance of NA in viral replication, the current anti-influenza treatments mainly target NA enzyme activity. However, this strategy has proven to be suboptimal as drug-resistant viral strains emerge shortly after the antiviral treatment. Although annual vaccines offer protection against influenza, the constant antigenic drift and shift of HA and NA proteins necessitate annual updating of virus strains, and mismatch between vaccines and the actual circulating viruses is

* This work was supported in part by the Canadian Regulatory Strategy for Biotechnology (to X. L.) and Canadian Institutes of Health Research Pandemic Preparedness Team Grant TPA-90188 (to E. G. B.).
[1] Supported by a fellowship from the Natural Sciences and Engineering Research Council of Canada.
[2] Supported by a scholarship from King Abdulaziz University through the Saudi Arabian Cultural Bureau in Canada.
[3] To whom correspondence should be addressed: Centre for Vaccine Evaluation, Health Canada, Sir F. G. Banting Research Centre, A/L 2201E, 251 Sir Frederick Banting Driveway, Ottawa, Ontario K1A 0K9, Canada. Tel.: 613-954-2383; Fax: 613-941-8933; E-mail: Sean.Li@hc-sc.gc.ca.

[4] The abbreviations used are: NA, neuraminidase; aa, amino acid(s); MDCK, Madin-Darby canine kidney; m.o.i., multiplicity of infection; MUNANA, 2-(4-methylumberlliferyl)-α-D-*N*-acetylneuraminic acid.

known to render the vaccines ineffective (17). These problems associated with current antiviral therapy and vaccines against influenza are directly related to the nature of the HA and NA proteins of which the antigenic epitopes are constantly changing in an unpredictable fashion as a result of viral replication error and gene reassortment in combination with constant immune pressure (10, 18, 19). Therefore, exploring the role of the highly conserved regions in HA and NA would be of unquestionable importance for a better understanding of the molecular mechanisms underlying viral pathogenesis and formulation of new antiviral regimen and vaccine development strategies.

Although many studies have reported the functional roles of conserved sequences in HA, fewer studies have been conducted on the conserved sequences of NA. Through a comprehensive bioinformatics analyses of all NA sequences in the GenBank™, we have recently identified a novel conserved peptide region in the NA protein (denoted HCA-2) with a conservation rate of nearly 100% (20, 21). In addition, HCA-2 monoclonal antibodies against this region were used for quantitative analysis of NA component in influenza vaccines (20). However, the specific function of this region remains unknown. In the current study, we aimed at elucidating the role of the HCA-2 amino acids (aa) in viral function. Our study reveals that this universally conserved epitope contributes significantly to efficient viral replication by maintaining favorable NA protein structure and substrate binding to maximize enzymatic activities.

EXPERIMENTAL PROCEDURES

Reagents—The NA plasmid from influenza A/PR8/34 (N1) was used to transfect 293-T cells with PR8 backbone plasmids (pHW191-PB2, pHW192-PB1, pHW193-PA, pHW194-HA, pHW195-NP, pHW197-M, and pHW198-NS) to generate recombinant viruses. The eight-plasmid reverse genetics system was kindly provided by Dr. Richard Webby (St. Jude Children's Research Hospital, Memphis, TN).

All viruses were rescued, amplified in 10-day-old embryonated chicken eggs, passaged three times (E3) in 10-day-old chicken eggs, and concentrated by centrifugation onto a 30% sucrose cushion. To ensure that no additional mutations occurred in the NA gene during generation or passaging, NA viral RNA was extracted from E3 viruses and then sequenced.

Madin-Darby canine kidney (MDCK) cells and human embryonic kidney (HEK) 293-T cells were obtained from the American Type Culture Collection (Manassas, VA). Cells were grown and cultured in Dulbecco's modified Eagle's medium (DMEM) as described previously (22).

Alanine Scanning Mutagenesis—To analyze the role of each of the aa residues within the universal epitope in virus replication, we made aa substitutions using alanine scanning mutagenesis, a technique used to rapidly identify residues important for protein function, stability, and shape. Each alanine substitution examines the contribution of an individual amino acid side chain to the functionality of the protein (23). We used a Stratagene mutagenesis kit (Mississauga, Ontario, Canada) to generate these substitution mutations in the NA gene. Primers were then designed to insert either substitution mutations or the deletion mutation. Mutagenesis was then performed according to the manufacturer's instructions.

Growth Curves—MDCK cells were inoculated with viral samples in serum-free DMEM at a high multiplicity of infection (m.o.i.) of 5 pfu/cell or a low m.o.i. of 0.001 for 1 h in the presence of 2 μg of L-1-tosylamido-2-phenylethyl chloromethyl ketone. The inoculum was removed by extensive washing with 0.9% NaCl in citric acid buffer and PBS thereafter. Next, serum-free DMEM with 2 μg/ml L-1-tosylamido-2-phenylethyl chloromethyl ketone-treated trypsin was then added to the inoculated cell monolayers. For the high m.o.i., supernatants were harvested every 1.5 h from time 0 h until time 9 h. For the low m.o.i., supernatant was harvested over a course of 72 h at time points 0, 6, 12, 18, 24, 36, 48, and 72 h. Growth curve analysis was performed in triplicates. Harvested medium was then titrated using a plaque assay as described previously (9).

NA Enzymatic Activity—NA enzymatic activity was measured by standardizing the samples with pfu as described (24). Virus was aliquoted at a titer of 1×10^7 pfu and then incubated at 37 °C with 2-(4-methylumberlliferyl)-α-D-*N*-acetylneuraminic acid (MUNANA). After 20 min, the reaction was stopped with 0.14 M NaOH and 83% ethanol, and NA activity was measured with an excitation of 360 nm and an emission of 448 nm (25). The analysis was performed in triplicate where the average activity of the wild type (WT) was set as 100% and the average activity of the other variants is expressed as a percentage of the WT. To assess K_m and V_{max}, virus samples were incubated with concentrations of MUNANA ranging from 0 to 1200 μM. Fluorescence was monitored every 60 s for 60 min. The K_m and V_{max} were calculated with GraphPad Prism software (GraphPad version 5; San Diego, CA) by fitting the data to the Michaelis-Menten equation using non-linear regression.

Thermostability of NA—The effect of temperature on NA function was determined by incubating the NA proteins for 15 min at various temperatures ranging from 36 to 54 °C (6). After incubation, NA activity was immediately determined using the MUNANA assay described above.

Protein Modeling—Mutations were homology-modeled against the influenza N1 crystal structure. Models were prepared for each mutation using the "automodel" module from Modeller software version 9.8 (26) and were superimposed with the wild type NA and inspected for impact on enzyme structure and sialic acid binding. Visualization and analysis were performed using the software UCSF Chimera (27). Alanine scanning mutations were homology-modeled against the influenza N1 crystal structure (Protein Data Bank code 1NN2) with the automodel module from Modeller version 9.8 (26). Homology models were superimposed with WT and inspected for impact on the neuraminidase structure and sialic acid binding. Structure superposition, visualization, and analysis were performed using UCSF Chimera (27).

Statistical Analyses—Two-way analysis of variance with the Bonferroni post-test was used to compare data between variants. All statistical analysis was conducted using GraphPad Prism software. p values <0.05 were considered statistically significant. Results are presented as the mean ± S.E.

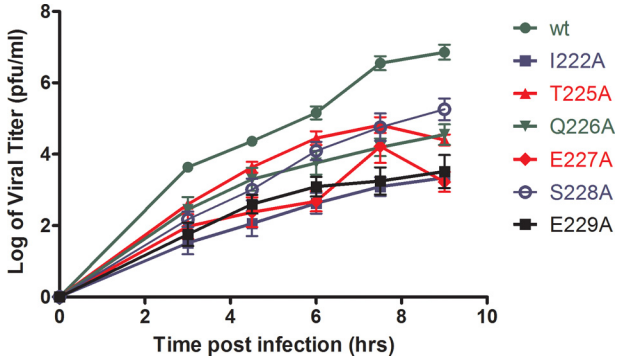

FIGURE 1. **High m.o.i. growth curve.** To determine single step virus growth, MDCK cells were infected with WT or mutants viruses at high m.o.i. (5). At various times postinfection (up to 9 h), the supernatants were collected for virus titration in a plaque assay. *Error bars* represent ±S.E. Two-way analysis of variance was used for significance comparison with a p value <0.05 being considered significant. * denotes a significant difference found between WT and the remainder of the variants.

TABLE 1
Rate of viral growth
The growth rate for the viruses was determined using the slope of the regression line from either the high m.o.i. or the low m.o.i. growth curves (43).

Viral variant	Rate of growth (high m.o.i.)	Rate of growth (low m.o.i.)
	log_{10} *pfu/ml/h*	log_{10} *pfu/ml/day*
WT	0.75 ± 0.012	2.35 ± 0.52
I222A	0.37 ± 0.014	1.32 ± 0.42
T225A	0.51 ± 0.042	1.49 ± 0.41
Q226A	0.49 ± 0.028	1.19 ± 0.46
E227A	0.39 ± 0.034	1.33 ± 0.41
S228A	0.59 ± 0.019	1.50 ± 0.49
E229A	0.38 ± 0.025	1.04 ± 0.26

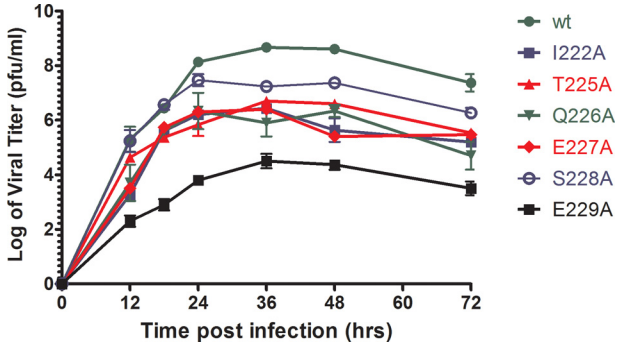

FIGURE 2. **Low m.o.i. growth curve.** To determine multiple rounds of infection, MDCK cells were infected with the WT or mutant virus at low m.o.i. (0.001). At various times postinfection (up to 75 h), the supernatants were collected for virus titration using a plaque assay. *Error bars* represent ±S.E. Two-way analysis of variance was used for significance comparison with a p value <0.05 being considered significant. * denotes a significant difference found between WT and the remainder of the variants.

RESULTS

The HCA-2 Region Is Essential to Virus Rescue—To determine the contribution of the universally conserved HCA-2 region to NA function, we substituted individual aa with alanine in the HCA-2 domain of the NA gene and analyzed the viability of the mutant viruses using the eight-plasmid reverse genetics system (28, 29). The successful rescue of virus was first determined by positive hemagglutination assay followed by plaque assay in conjunction with viral RNA detection. If samples showed negativity in hemagglutination, plaque formation, and viral RNA detection, they were thus deemed as being unable to be rescued. These experiments showed that substitution of Leu-223, Arg-224, or Cys-230 with alanine is lethal to virus survival, revealing critical roles for these amino acids in viral replication. Moreover, transfectant viruses missing the entire HCA-2 region were also found to be not rescuable, further confirming that this region is necessary for production of infectious virus. Other mutants including I222A, T225A, Q226A, E227A, S228A, and E229A substitutions were generated. Sequencing of viral RNA extracted from these variants confirmed the presence of the substitutions and the absence of any additional mutations in other regions of the NA after passaging.

The HCA-2 Region Affects Viral Spread and Growth Kinetics—To compare the growth kinetics of these viral variants, we infected the cells with viruses at high and low m.o.i. because the high m.o.i. response would determine the single round viral replication whereas the low m.o.i. curve could reveal multiple cycles of viral growth and spread. Specifically, MDCK cells were inoculated for 1 h with either a high m.o.i. of 5 or a low m.o.i. of 0.001 to examine the role of this region in viral replication.

As shown in the high m.o.i. growth curve (Fig. 1), the rate of viral growth for the WT was significantly better than the rate of all other NA variants with values of growth rates presented in Table 1. It is of note that the difference between the mutants and the WT is more pronounced when low m.o.i. (Fig. 2) was used to inoculate the culture (Table 1). Although T225A and S228A grew at a higher rate than the other mutants, the difference between the WT and all mutants was much more drastic. Taken together, all of the NA variants grew much less effectively than the WT, and substitutions at Leu-223, Arg-224, and Cys-230 with alanine were found to be lethal.

The HCA-2 Region Significantly Alters NA Enzymatic Activity and Substrate Binding—We next determined whether the decreased levels of viral progeny following the infection with mutant viruses were associated with altered enzymatic activities in these mutants. The NA enzymatic activities of all mutants showed significantly lower activities compared with the WT as shown in Fig. 3. It is also of note that the lower activities in the mutants were largely in agreement with the viral growth data (Figs. 1 and 2).

To better shed light on the molecular mechanism underlying the altered enzymatic activities in the various mutants, we determined the K_m and V_{max}, which reflect the affinity of the enzyme for the substrate and maximum rate a reaction can occur when the enzyme is fully saturated with substrate, respectively. As shown in Fig. 4, the WT enzyme has a more efficient rate of converting the substrate to the final products. To get insight into the fundamental parameters of enzyme kinetics, the enzyme reaction data of reaction velocity relative to substrate concentration were then used to calculate for K_m and V_{max}, which are presented in Table 2. Here it is shown that the WT has a significantly smaller K_m and larger V_{max} compared with all of the mutants; specifically, the WT K_m value is ~40 μM compared with 122–253 μM for the mutants, suggesting that mutation in this region resulted in decreased affinity for sialic acid substrate. Moreover, the smaller V_{max} values of the mutants represent the diminished rates of enzyme catalysis as a result of mutations in this region. This difference in the K_m and

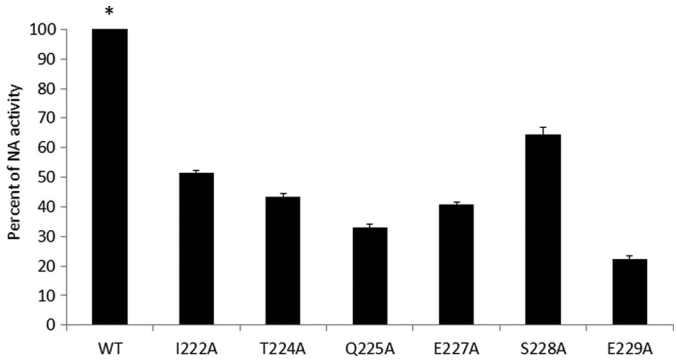

FIGURE 3. **Measurements of NA enzymatic activities.** Experiments were performed in triplicates with *error bars* representing ±S.E. Two-way analysis of variance was used for significance comparison with a p value <0.05 being considered significant. * denotes a significant difference found between WT and the remainder of the variants.

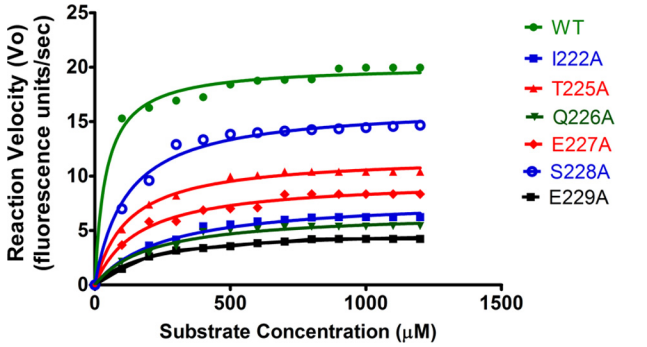

FIGURE 4. **Enzymatic kinetics study on WT and variants.** Fluorescence of MUNANA was measured at concentrations of 0–1200 mM every 60 s for 60 min. Velocity is expressed in terms of fluorometric units/s. Data shown represent one of three experiments conducted on three different occasions.

TABLE 2

K_m and V_{max} of viral variants

Values are derived from three separate runs of experiments; ± represents standard S.D.

Variant	V_{max}	K_m	V_{max}/K_m	-Fold[a]
	units/s	*μM*		
WT	20.85 ± 0.32	40.88 ± 6.55	0.51	1
I222A	7.975 ± 0.38	253.2 ± 41.95	0.03	0.06
T225A	11.85 ± 0.19	122.4 ± 10.22	0.09	0.09
Q226A	6.656 ± 0.27	209.8 ± 32.26	0.03	0.03
E227A	9.658 ± 0.27	162.2 ± 19.78	0.05	0.05
S228A	16.48 ± 0.38	117.8 ± 14.26	0.13	0.13
E229A	5.097 ± 0.10	201.3 ± 15.18	0.02	0.02

[a] The ratio of V_{max}/K_m is arbitrarily set as 1 with the values of the mutants being expressed against that of the WT (44).

V_{max} in the mutants is also noted, although it is not as marked as that compared with the WT. Indeed, the WT is far more potent of an enzyme, being 7.6 times more effective, when the V_{max}/K_m ratio is considered than S228A, a mutant that possessed the best viral replication among all HCA-2 region mutants. Apparently, the difference in the viral growth and Michaelis-Menten kinetics among the viral mutants may be due to varying degrees of structural changes in the NA proteins induced by the individual aa substitution (see below for more discussion). Nevertheless, data from these enzymatic studies are largely in agreement with the viral replication data in Figs. 1 and 2.

In short, data from enzymatic kinetics analyses (Table 2) are largely in agreement with the growth rates of the mutant and WT viruses. Specifically, whereas S228A and T225A are slightly more efficient enzymatically, all mutants are not as effective as the WT NA enzyme.

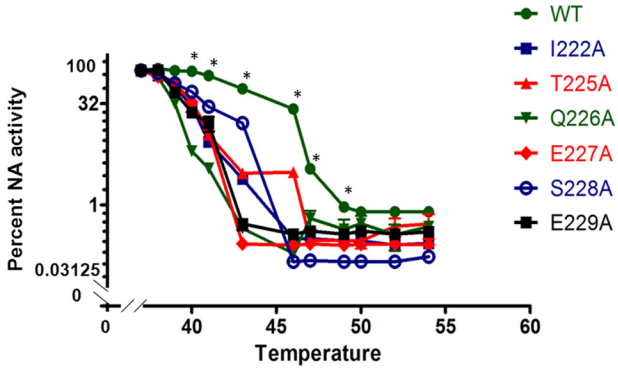

FIGURE 5. **Thermostability of viral variants.** WT and mutant viruses were incubated at various temperatures for 15 min, and the samples were then used in a standard MUNANA assay to measure NA activity. 100% activity was arbitrarily set for each individual enzyme itself at 37 °C, not against the wild type. Experiments were performed in triplicate. * signifies $p < 0.05$, and *error bars* represent S.E.

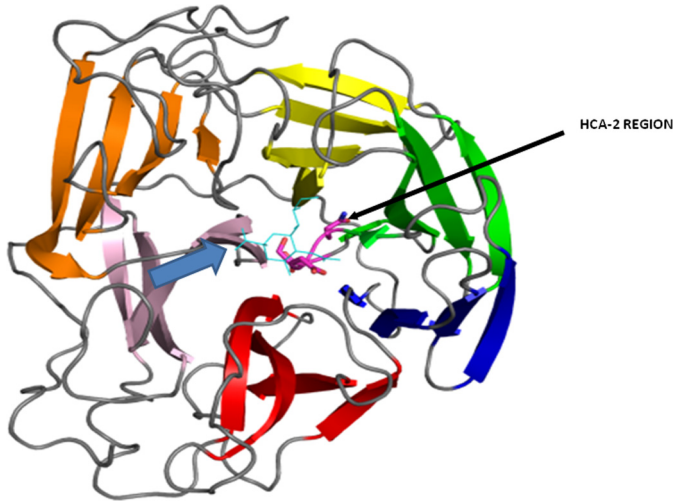

FIGURE 6. **Location of the universal sequence (HCA-2) in WT NA.** The region 226–229 (*magenta*) resides in the central core of the neuraminidase protein; the rest of the aa in HCA-2 could not be seen in the particular graph (see below for details). The *blue arrow* points to the sialic acid substrate (*cyan*).

The Mutant NA Enzymes Are More Thermolabile—Having observed decreased substrate binding and enzyme activities in the mutants, we next wished to assess how the tertiary structures of these mutants could have been altered. To this end, we investigated the thermostability of these mutants by heating the proteins at various temperatures and measuring the activity using a procedure described previously (6). As shown in Fig. 5, all mutant NA proteins were significantly more thermolabile than the WT as measured as a function of enzymatic activity following heat treatment, suggesting that the tertiary structures of these mutants were less stable, constituting a suboptimal environment for NA protein function.

Protein Modeling—Given that previous studies on the crystal structure of NA were focused on the amino acids within the enzymatic region and substrate binding pocket (10, 30, 31), we next used protein modeling to analyze how each of the aa contributed to NA structural integrity.

Fig. 6 illustrates the universal sequence (HCA-2) in the WT NA. Four of the amino acids studied (226–229) (colored in

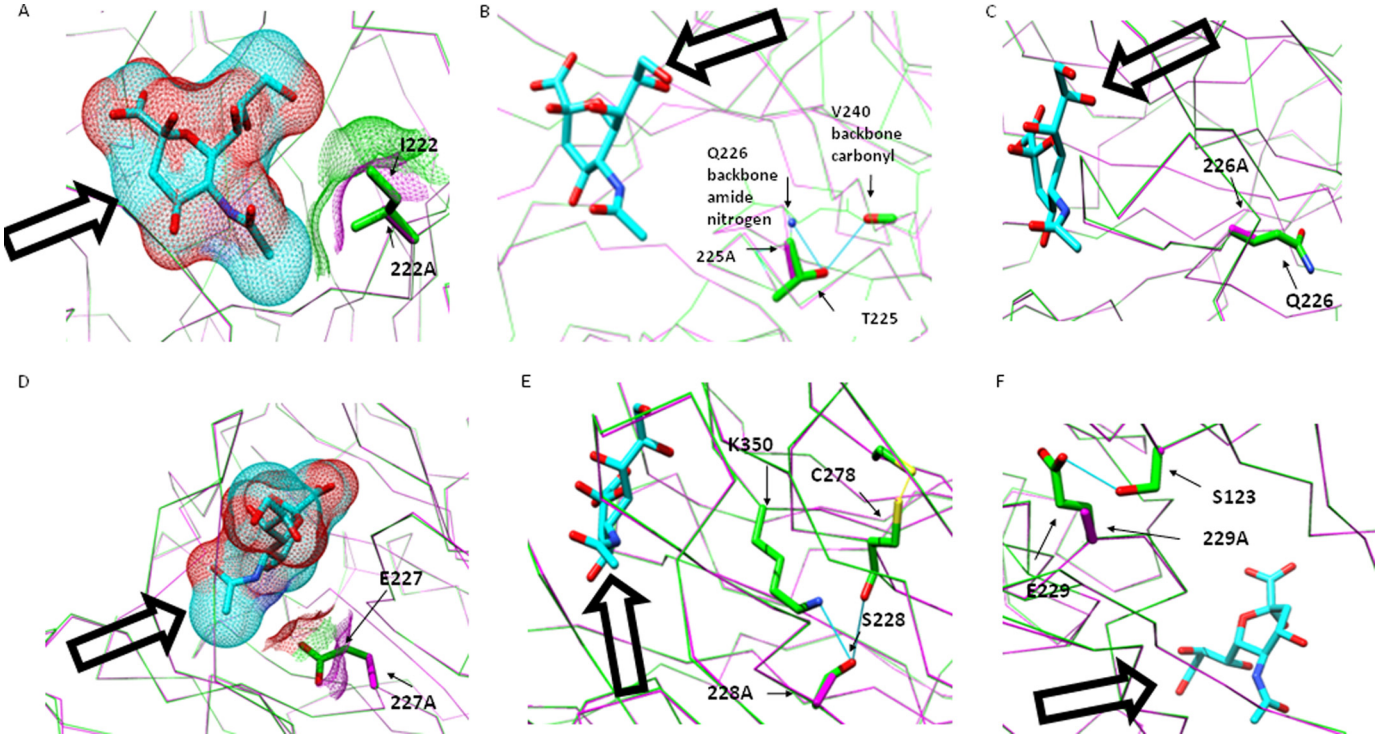

FIGURE 7. **The effects of substitution on protein structure.** In all panels, the *open arrows* indicate the sialic acid substrates. *A*, Ile-222 (*green*) creates a hydrophobic contact with the methyl group on the sialic acid, and substitution of the isoleucine residue with an alanine (*magenta*) reduces the hydrophobic contact area available for binding with the sialic acid. *B*, the Thr-225 side chain (*green*) is directed toward the neuraminidase core and participates in stabilizing a β-sheet by making a hydrogen bond with the Val-240 backbone carboxyl. The T225A mutation abolishes these H-bonds, possibly destabilizing the β-sheet. *C*, the Q226A mutation results in a reduced side chain volume. *D*, the Glu-227 side chain carboxyl group makes a polar contact with the sialic acid, and mutation of this residue to alanine reduces the available binding surface area to sialic acid and abolishes the polar contact area. *E*, Ser-228 resides in the center of the protein, and mutation of this residue abolishes hydrogen bonds from the serine side chain hydroxyl oxygen to Lys-350 and the Cys-278. *F*, S229A could result in the loss of one hydrogen bond from the Glu-229 side chain carboxyl oxygen to the Ser-123 side chain hydroxyl group.

magenta and indicated by the *arrow*) reside in the central core of the molecule (Fig. 6) (32). Our analyses revealed that substitutions of the aa in this highly conserved region could have profound effects on the structural integrity of substrate enzyme binding. Specifically, as shown in Fig. 7*A*, Ile-222 (*green*) directly binds to the substrate (indicated by *open arrow*) by creating a hydrophobic contact with the methyl group on the sialic acid, and substitution of the isoleucine residue with an alanine (*magenta*) reduces the hydrophobic contact area available for binding with the sialic acid. The side chain of Thr-225 (colored in *green* as shown in Fig. 7*B*) is directed toward the neuraminidase core and participates in stabilizing a β-sheet by making a hydrogen bond with the Val-240 backbone carboxyl. The T225A mutation abolishes these H-bonds, possibly destabilizing the β-sheet. Gln-226 (colored in *green* in Fig. 7*C*) directly constitutes part of a β-sheet. It is likely that the Q226A mutation results in a reduced side chain volume (Fig. 7*C*), generating a large internal cavity and potentially destabilizing the internal structure. As far as Glu-227 is concerned, it is known to directly bind to the substrate; specifically, its side chain carboxyl group makes a polar contact with the sialic acid, and mutation of this residue to alanine reduces the available binding surface area to sialic acid and abolishes the polar contact area, thus weakening the binding with the substrate (Fig. 7*D*). Fig. 7*E* depicts the effect of S228A mutation. Ser-228 (*green*) resides in the center of the protein, and mutation of this residue abolishes hydrogen bonds from the serine side chain hydroxyl oxygen to Lys-350 and the Cys-278 (Fig. 7*E*), thus disrupting the internal structure needed for protein stability. Finally, Glu-229 (*green*) forms hydrogen bonds with Ser-123 (Fig. 7*F*). E229A mutation could result in the loss of one hydrogen bond from the Glu-229 side chain carboxyl oxygen to the Ser-123 side chain hydroxyl group. Taken together, these modeling analyses of NA structure indicate that the universally conserved sequence either is directly involved in binding to the substrate or contributes to the intermolecule bonds necessary for optimal catalytic reaction by the NA protein.

DISCUSSION

The ever evolving nature of influenza viral HA and NA is well known and presents daunting challenges for scientific and medical communities in achieving the objective to prevent and treat influenza disease. Identifying the conserved sequences in HA and NA and investigating their potential roles in viral pathogenesis are of critical importance to explore a new antiviral target and vaccine component. Although there here have been many studies on HA, many fewer studies have been conducted on NA. Specifically, the only universally conserved sequence of HA is found to be the fusion peptide (17), and antibodies against the fusion peptide demonstrated neutralizing activities against diverse strains of virus (33). There are also reports showing antibodies with a wide range of cross-neutralizing activity against conformational epitopes in HA (34–38). However, studies on NA in these areas have been very limited

with no report on the potential role of the highly or universally conserved sequence of NA in virus replication and its potential as a novel vaccine component. Our previous studies have revealed that aa 222–230 represent the only universally conserved sequence in NA with a conservation rate close to 100%; antibodies generated against this region could be used for quantitative analyses of NA components in vaccine preparation (17). However, how this sequence affects viral enzymatic activity and viral replication remains unknown. Clearly, investigation of the functional role of the only universally conserved sequence in the viral NA would be of unquestionable importance for a better understanding of influenza viral pathogenicity and formulation of new preventative and therapeutic strategies.

Given the proximity of this sequence to the enzyme active site, we hypothesized that it could be critically important for efficient virus replication by maintaining the structural integrity of the enzyme. Indeed, the decreased growth of all rescued mutants was found to be associated with significantly reduced enzymatic activity. Although these data reinforce the notion that enzymatic activity is positively associated with viral growth, our subsequent enzymatic analyses shed light on how the aa in this region are needed for NA protein to maintain its structural conformation necessary for maximal enzymatic activity. Specifically, in the enzymatic kinetics studies, the smaller values of K_m in the mutants indicate their decreased affinity in NA binding to the substrate, which may translate into much less effective conversion of substrates into final products as suggested by a substantially reduced ratio of V_{max}/K_m (Table 2), and this decreased substrate binding ultimately resulted in decreased viral growth rate (Table 1). Furthermore, the thermolabile properties of these mutants yield additional evidence that aa in this region are indispensable to constitute an optimal tertiary environment needed for maximal enzymatic activities.

The data from biological and biochemical analyses are consistent with the findings of protein modeling, which helps shed light on the molecular mechanisms underlying the contribution of the universal sequence to viral propagation. Specifically, it explains the mechanism for the loss of replication capabilities in I222A and E227A viruses because both Ile-222 and Glu-227 directly interact with the sialic acid substrate. Furthermore, although Thr-225, Gln-226, Ser-228, and Glu-229 do not directly interact with the sialic acid substrate, substitution of these amino acids with alanine resulted in significant loss of NA activity and decreased viral growth. As protein modeling suggested, it is likely that the primary effect of these substitutions is to abolish internal hydrogen bonding, thereby generating cavities and destabilizing the tertiary structure of the NA protein. Although globular proteins can tolerate internal cavities, they are less energetically favorable than closely packed arrangements. Therefore, it is possible that the introduction of these cavities by alanine substitution may perpetuate a structural reconfiguration to reduce the size of this internal cavity and thus distort the active site, similar to observations made in other protein studies (39–42). This distortion likely decreases the ability of the enzyme to bind and convert substrate into final products, thus ultimately hindering viral growth.

Although the data from the analyses of mutants in viral growth, enzymatic efficiency, and protein stability experiments are largely in agreement with one another, the difference among the mutants is not as drastic as that between the WT and all mutants. At this time, we are unable to explain the functional variations that existed between the different mutants; these are currently under further investigation in our laboratories. Regardless, our work clearly reveals that this unique sequence is crucially important for binding to the substrate and stabilizing the native tertiary structure favorable for maximal enzymatic activity and viral propagation. These findings could help evaluate the validity of this epitope as an attractive target for antiviral intervention and universal vaccine development, particularly given that it is the only conserved sequence among all influenza viral NA proteins.

Acknowledgments—We are indebted to Dr. Ajoy Basak (Ottawa Hospital Research Institute) and Dr. John Mark (Health Canada) for helpful discussions. We thank Michele Lemieux and Monica Tocchi for technical assistance. Monika Tocchi is also acknowledged for editorial assistance.

REFERENCES

1. Baker, A. T., Varghese, J. N., Laver, W. G., Air, G. M., and Colman, P. M. (1987) Three-dimensional structure of neuraminidase of subtype N9 from an avian influenza virus. *Proteins* **2,** 111–117
2. Webster, R. G., and Bean, W. J., Jr. (1978) Genetics of influenza virus. *Annu. Rev. Genet.* **12,** 415–431
3. Tong, S., Li, Y., Rivailler, P., Conrardy, C., Castillo, D. A., Chen, L.M., Recuenco, S., Ellison, J. A., Davis, C. T., York, I. A., Turmelle, A. S., Moran, D., Rogers, S., Shi, M., Tao, Y., Weil, M. R., Tang, K., Rowe, L. A., Sammons, S., Xu, X., Frace, M., Lindblade, K. A., Cox, N. J., Anderson, L. J., Rupprecht, C. E., and Donis, R. O. (2012) A distinct lineage of influenza A virus from bats. *Proc. Natl. Acad. Sci. U.S.A.* **109,** 4269–4274
4. Skehel, J. J., and Wiley, D. C. (2000) Receptor binding and membrane fusion in virus entry: the influenza hemagglutinin. *Annu. Rev. Biochem.* **69,** 531–569
5. Air, G. M., and Laver, W. G. (1989) The neuraminidase of influenza virus. *Proteins* **6,** 341–356
6. Palese, P., Tobita, K., Ueda, M., and Compans, R. W. (1974) Characterization of temperature sensitive influenza virus mutants defective in neuraminidase. *Virology* **61,** 397–410
7. Griffin, J. A., Basak, S., and Compans, R. W. (1983) Effects of hexose starvation and the role of sialic acid in influenza virus release. *Virology* **125,** 324–334
8. Liu, C., Eichelberger, M. C., Compans, R. W., and Air, G. M. (1995) Influenza type A virus neuraminidase does not play a role in viral entry, replication, assembly, or budding. *J. Virol.* **69,** 1099–1106
9. Hashem, A. M., Flaman, A. S., Farnsworth, A., Brown, E. G., Van Domselaar, G., He, R., and Li, X. (2009) Aurintricarboxylic acid is a potent inhibitor of influenza A and B virus neuraminidases. *PLoS One* **4,** e8350
10. Colman, P. M., Varghese, J. N., and Laver, W. G. (1983) Structure of the catalytic and antigenic sites in influenza virus neuraminidase. *Nature* **303,** 41–44
11. Klenk, H. D., and Rott, R. (1988) The molecular biology of influenza virus pathogenicity. *Adv. Virus Res.* **34,** 247–281
12. Ohuchi, M., Asaoka, N., Sakai, T., and Ohuchi, R. (2006) Roles of neuraminidase in the initial stage of influenza virus infection. *Microbes Infect.* **8,** 1287–1293
13. Su, B., Wurtzer, S., Rameix-Welti, M. A., Dwyer, D., van der Werf, S., Naffakh, N., Clavel, F., and Labrosse, B. (2009) Enhancement of the influenza A hemagglutinin (HA)-mediated cell-cell fusion and virus entry by the viral neuraminidase (NA). *PLoS One* **4,** e8495
14. Peltola, V. T., and McCullers, J. A. (2004) Respiratory viruses predisposing to bacterial infections: role of neuraminidase. *Pediatr. Infect. Dis. J.* **23,** S87–S97

15. McCullers, J. A. (2011) Preventing and treating secondary bacterial infections with antiviral agents. *Antivir. Ther.* **16,** 123–135
16. Govorkova, E. A., and McCullers, J. A. (2013) Therapeutics against influenza. *Curr. Top. Microbiol. Immunol.* **370,** 273–300
17. Chun, S., Li, C., Van Domselaar, G., Wang, J., Farnsworth, A., Cui, X., Rode, H., Cyr, T.D., He, R., and Li, X. (2008) Universal antibodies and their applications to the quantitative determination of virtually all subtypes of the influenza A viral hemagglutinins. *Vaccine* **26,** 6068–6076
18. Colman, P. M. (1992) Structural basis of antigenic variation: studies of influenza virus neuraminidase. *Immunol. Cell Biol.* **70,** 209–214
19. Laver, W. G. (1984) Antigenic variation and the structure of influenza virus glycoproteins. *Microbiol. Sci.* **1,** 37–43
20. Gravel, C., Li, C., Wang, J., Hashem, A. M., Jaentschke, B., Xu, K. W., Lorbetskie, B., Gingras, G., Aubin, Y., Van Domselaar, G., Girard, M., He, R., and Li, X. (2010) Qualitative and quantitative analyses of virtually all subtypes of influenza A and B viral neuraminidases using antibodies targeting the universally conserved sequences. *Vaccine* **28,** 5774–5784
21. Varghese, J.N., Laver, W.G., and Colman, P.M. (1983) Structure of the influenza virus glycoprotein antigen neuraminidase at 2.9 Å resolution. *Nature* **303,** 35–40
22. Hashem, A., Jaentschke, B., Gravel, C., Tocchi, M., Doyle, T., Rosu-Myles, M., He, R., and Li, X. (2012) Subcutaneous immunization with recombinant adenovirus expressing influenza A nucleoprotein protects mice against lethal viral challenge. *Hum. Vaccin. Immunother.* **8,** 425–430
23. Morrison, K. L., and Weiss, G. A. (2001) Combinatorial alanine-scanning. *Curr. Opin. Chem. Biol.* **5,** 302–307
24. Ilyushina, N. A., Bovin, N. V., and Webster, R. G. (2012) Decreased neuraminidase activity is important for the adaptation of H5N1 influenza virus to human airway epithelium. *J. Virol.* **86,** 4724–4733
25. Potier, M., Mameli, L., Bélisle, M., Dallaire, L., and Melançon, S. B. (1979) Fluorometric assay of neuraminidase with a sodium (4-methylumbelliferyl-α-D-N-acetylneuraminate) substrate. *Anal. Biochem.* **94,** 287–296
26. Eswar, N., Webb, B., Marti-Renom, M.A., Madhusudhan, M.S., Eramian, D., Shen, M.Y., Pieper, U., and Sali, A. (2006) Comparative protein structure modeling using Modeller. *Curr. Protoc. Bioinformatics* **Chapter 5,** Unit 5.6
27. Pettersen, E.F., Goddard, T.D., Huang, C.C., Couch, G.S., Greenblatt, D.M., Meng, E.C., and Ferrin, T.E. (2004) UCSF Chimera—a visualization system for exploratory research and analysis. *J. Comput. Chem.* **25,** 1605–1612
28. Hoffmann, E., Neumann, G., Kawaoka, Y., Hobom, G., and Webster, R.G. (2000) A DNA transfection system for generation of influenza A virus from eight plasmids. *Proc. Natl. Acad. Sci. U.S.A.* **97,** 6108–6113
29. Liu, Q., Wang, S., Ma, G., Pu, J., Forbes, N.E., Brown, E.G., and Liu, J.H. (2009) Improved and simplified recombineering approach for influenza virus reverse genetics. *J. Mol. Genet. Med.* **3,** 225–231
30. Colman, P.M., Laver, W.G., Varghese, J.N., Baker, A.T., Tulloch, P.A., Air, G.M., and Webster, R.G. (1987) Three-dimensional structure of a complex of antibody with influenza virus neuraminidase. *Nature* **326,** 358–363
31. Colman, P.M., Tulip, W.R., Varghese, J.N., Tulloch, P.A., Baker, A.T., Laver, W.G., Air, G.M., and Webster, R.G. (1989) Three-dimensional structures of influenza virus neuraminidase-antibody complexes. *Philos. Trans. R. Soc. Lond. B Biol. Sci.* **323,** 511–518
32. Colman, P.M. (1994) Influenza virus neuraminidase: structure, antibodies, and inhibitors. *Protein Sci.* **3,** 1687–1696
33. Hashem, A.M., Van Domselaar, G., Li, C., Wang, J., She, Y.M., Cyr, T.D., Sui, J., He, R., Marasco, W.A., and Li, X. (2010) Universal antibodies against the highly conserved influenza fusion peptide cross-neutralize several subtypes of influenza A virus. *Biochem. Biophys. Res. Commun.* **403,** 247–251
34. Corti, D., Voss, J., Gamblin, S. J., Codoni, G., Macagno, A., Jarrossay, D., Vachieri, S. G., Pinna, D., Minola, A., Vanzetta, F., Silacci, C., Fernandez-Rodriguez, B. M., Agatic, G., Bianchi, S., Giacchetto-Sasselli, I., Calder, L., Sallusto, F., Collins, P., Haire, L. F., Temperton, N., Langedijk, J. P., Skehel, J. J., and Lanzavecchia, A. (2011) A neutralizing antibody selected from plasma cells that binds to group 1 and group 2 influenza A hemagglutinins. *Science* **333,** 850–856
35. Ekiert, D. C., Bhabha, G., Elsliger, M. A., Friesen, R. H., Jongeneelen, M., Throsby, M., Goudsmit, J., and Wilson, I. A. (2009) Antibody recognition of a highly conserved influenza virus epitope. *Science* **324,** 246–251
36. Ekiert, D.C., Friesen, R.H., Bhabha, G., Kwaks, T., Jongeneelen, M., Yu, W., Ophorst, C., Cox, F., Korse, H. J., and Brandenburg, B. (2011) A highly conserved neutralizing epitope on group 2 Influenza A viruses. *Science* **333,** 843–850
37. Sui, J., Hwang, W. C., Perez, S., Wei, G., Aird, D., Chen, L. M., Santelli, E., Stec, B., Cadwell, G., and Ali, M. (2009) Structural and functional bases for broad-spectrum neutralization of avian and human influenza A viruses. *Nat. Struct. Mol. Biol.* **16,** 265–273
38. Wei, C. J., Yassine, H. M., McTamney, P. M., Gall, J. G., Whittle, J. R., Boyington, J. C., and Nabel, G. J. (2012) Elicitation of broadly neutralizing influenza antibodies in animals with previous influenza exposure. *Sci. Transl. Med.* **4,** 147ra114
39. Lim, W. A., Farruggio, D. C., and Sauer, R. T. (1992) Structural and energetic consequences of disruptive mutations in a protein core. *Biochemistry* **31,** 4324–4333
40. Fuchs, W., Backovic, M., Klupp, B. G., Rey, F. A., and Mettenleiter, T. C. (2012) Structure-based mutational analysis of the highly conserved domain IV glycoprotein H of pseudorabies virus. *J. Virol.* **86,** 8002–8013
41. Monera, O. D., Sönnichsen, F. D., Hicks, L., Kay, C. M., and Hodges, R. S. (1996) The relative positions of alanine residues in the hydrophobic core control the formation of two-stranded or four-stranded α-helical coiled-coils. *Protein Eng.* **9,** 353–363
42. Xu, B., Hua, Q. X., Nakagawa, S. H., Jia, W., Chu, Y. C., Katsoyannis, P. G., and Weiss, M. A. (2002) A cavity-forming mutation in insulin induces segmental unfolding of a surrounding α-helix. *Protein Sci.* **11,** 104–116
43. Hatta, Y., Hershberger, K., Shinya, K., Proll, S. C., Dubielzig, R. R., Hatta, M., Katze, M. G., Kawaoka, Y., and Suresh, M. (2010) Viral replication rate regulates clinical outcome and CD8 T cell responses during highly pathogenic H5N1 influenza virus infection in mice. *PLoS Pathog.* **6,** e1001139
44. Basak, A., Chrétien, M., and Seidah, N. (2002) A rapid fluorometric assay for the proteolytic activity of SKI-1/S1P based on the surface glycoprotein of the hemorrhagic fever Lassa virus. *FEBS Lett.* **514,** 333–339